Use of Electrochemistry To Predict Ethylene Absorption Capacities of Reactive Absorption Systems

T. A. Reine, W. M. Edwards, B. Wang, J. J. Lagowski, and R. B. Eldridge*

Department of Chemical Engineering, The Separations Research Program, The University of Texas at Austin, Austin, Texas 78712-1062

The ethylene absorption capacities of six nonaqueous reactive absorption solutions have been investigated by cyclic voltammetry and equilibrium cell experiments. Validation of the electrochemical method as a novel screening technique for ethylene-absorbing solutions was accomplished by qualitative comparison to equilibrium cell results. Metal salt−ligand pairs included combinations of cuprous chloride and cuprous bromide salts with pyridine, benzylamine, and aniline. The cyclic voltammetry experiments at 0.01 M copper concentration included multiple ligand concentrations over a range of scan rates to identify trends in ethylene complexation. Equilibrium cell experiments near 1 M copper were useful in examining chemical and physical effects as well as quantifying the ethylene capacity of the solutions at higher metal loadings. Results from both techniques suggested that the solution with the best ethylene capacity consisted of cuprous chloride with aniline ligand.

Introduction

The recovery of extremely pure olefins from a mixed stream containing olefins and paraffins is of primary importance in the chemical industry. To achieve the high degree of purity necessary for commercial-grade ethylene, the close boiling mixture of ethylene and ethane is presently separated by cryogenic distillation in towers with up to 150 trays operated at pressures up to 400 psi and temperatures as low as −90 °C.[1] For this reason, the economy of scale often forces smaller streams that are produced distant from the distillation train to be burned as refinery fuel or flared, creating both a loss of potential value and/or harmful environmental implications. Alternative methods of olefin/paraffin separation certainly hold an enormous potential for capital and energy cost savings. Many alternatives have been investigated including membranes, extractive distillation, adsorption, and (reactive and nonreactive) absorption; however, none of these has been implemented effectively on an industrial scale.[2]

For the case of reactive absorption, complexation of the olefin with a transition metal (traditionally silver or copper) has been the most extensively studied approach. A review of this technique given by Safarik and Eldridge[3] offered a set of criteria for a desired absorption solvent. The primary characteristic of a good absorption solvent is a high capacity and selectivity for the olefin. In this present work, we examine different liquid absorption systems' capacities to absorb ethylene using two distinct methods for evaluation. The first is a novel fast screening technique using benchtop electrochemistry to qualitatively compare different systems, and the second is the commonly used stirred equilibrium cell to quantitatively define the olefin capacity. The first technique was validated by comparison to the well-established second technique for key cases.

* To whom correspondence should be addressed. Tel.: (512) 471-7067. Fax: (512) 471-1720. E-mail: rbeldr@che.utexas.edu.

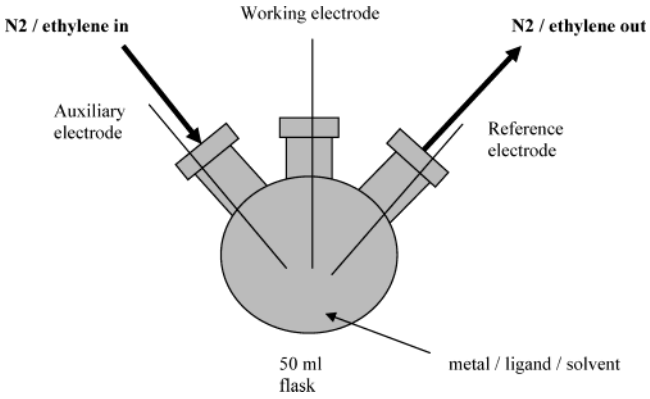

Figure 1. CV experimental setup.

Experimental Section

Cyclic voltammetry (CV) was utilized to examine the qualitative changes in the redox properties of the Cu(II)/Cu(I) and Cu(I)/Cu couples in equilibrium with 1 atm of N_2 and with 1 atm of C_2H_4 by bubbling the appropriate gas through the solution containing the metal ion for 30 min. Electrochemical measurements were carried out using an EG&G Princeton Applied Research (PAR) potentiostat/galvanostat (model 273A) controlled with the PAR 270 software package and a three-electrode cell at room temperature. The experimental setup shown in Figure 1 consists of a platinum disk as the working electrode, a platinum wire as the counter electrode, and a silver wire as the reference electrode.

The general experimental protocol involved establishing the CV curve for the copper ion in a given environment by first saturating the environment with oxygen-free nitrogen, which was produced by passing the research-grade gas (assay, 99.9999%) over a column of BASF catalyst. After the base voltammogram was established in the nitrogen-saturated environment, the gas flow through the system was switched to ethylene, and complexes between the metal ion and the ethylene were observed by a shift in the half-wave potential. The difference between the CVs under these conditions

10.1021/ie049917n CCC: $27.50
Published on Web 08/25/2004

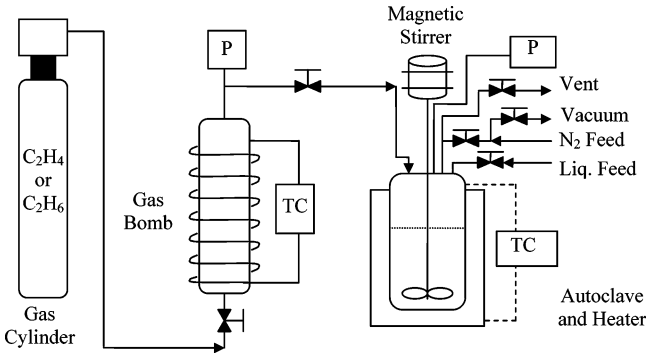

Figure 2. Autoclave experimental setup.

reflects the capacity of the environment to form olefin complexes. The magnitude of the shift of the half-wave potential corresponds to the environment's capacity to absorb ethylene.

Cuprous salts of chloride and bromide from Acros Organics at 97% and 98% purity, respectively, were used in the study. For all CV experiments, a metal salt concentration of 0.01 M was used. Using large metal concentrations is not appropriate for CV because the success of the experiment depends on the local depletion of the particular metal ion around the electrode. On the other hand, a large metal concentration is desired for practical ethylene absorption applications, so it is worth noting that these exact CV systems are not useful unless the results can be applied to concentrated metal solutions as well. Coordinating ligands for the metal ion included pyridine and aniline from Fisher Chemical at 99.9% purity and benzylamine (BzA) from Acros Organics at 99% purity. The supporting electrolyte necessary for the success of the technique was tetrabutylammonium perchlorate at 0.1 M, and the solvent used for dilution where appropriate was dimethylformamide (DMF) from Fisher Chemical at 99.9% purity.

The quantitative olefin capacity measurements were performed using a 500 cm^3 stainless steel autoclave from Autoclave Engineers with a magnetically coupled stirrer. The experimental setup shown in Figure 2 was designed by following similar systems in the literature.[4,5] The autoclave was connected via a shutoff valve to a 1 gal stainless steel gas bomb whose exact volume was previously measured by water volumes. Both the gas bomb and the autoclave were equipped with MKS pressure transducers, internal Omega thermocouples, and temperature controllers. The bomb was wrapped with heat tape and 3-in. pipe insulation, and the autoclave had an exterior fitted ceramic band heater. To begin the experiments, a weighed amount of a liquid absorption solution was charged into the autoclave, and then gas from the gas bomb (ethylene or ethane gas from Air Liquide at 98.5% purity) was charged while recording the initial conditions.

After the gas from the gas bomb was added to the autoclave, the system was stirred for a long enough period of time for the components to reach equilibrium. The pressure and temperature measurements along with the calculated vessel volumes were used with the three-parameter Prausnitz and Pitzer correlation[6] to calculate the number of moles of gas charged to the autoclave from the gas bomb and the number of moles of gas absorbed by the liquid solution. The system was maintained under a nitrogen environment (Air Liquide with 99.9% purity) while experiments were not being performed.

Theory

The change in the half-wave potential $\Delta E_{1/2}$ as a result of complexation can be described by the following equilibrium reactions. For any metal complexation reaction, the half-wave potential is shifted because of the creation of the new complex bonds requiring a fraction of the electrons from the metal cation. Given a different electron density on the central cation, a different amount of energy is needed to reduce the metal before and after the olefin complexation.[7] For the monovalent metal ion [Cu(I)/Cu(0) couple], the reduction reaction is

$$Cu^+ + e^- \leftrightarrow Cu \tag{1}$$

The Nernst equation for this reaction is given by

$$E = E^0 + \frac{RT}{nF} \ln \frac{a(Cu^+)}{a(Cu)} = E^0 + \frac{RT}{nF} \ln a(Cu^+) \tag{2}$$

where a(Cu) is taken as unity. The complexation reaction of ethylene is

$$Cu^+ + xC_2H_4 \leftrightarrow Cu^+(C_2H_4)_x \tag{3}$$

where the equilibrium expression is

$$K_{eq} = \frac{a[Cu^+(C_2H_4)_x]}{a(Cu^+)\, a(C_2H_4)^x} \tag{4}$$

Combining reactions 1 and 3 gives the reduction reaction for the complex ion

$$Cu^+(C_2H_4)_x + e^- \leftrightarrow Cu + xC_2H_4 \tag{5}$$

The Nernst equation for this reaction is obtained by combining eqs 2 and 4.

$$E = E^0 + \frac{RT}{nF} \ln \frac{a[Cu^+(C_2H_4)_x]}{a(C_2H_4)^x K_{eq}} \tag{6}$$

By assuming a large concentration of ethylene compared to metal ions and nearly equivalent diffusion coefficients for the metal ion and its complex with ethylene, eq 6 can be shown to give a shift in the half-wave potential $\Delta E_{1/2}$ (eq 7).[8] From the CV experiment, the half-wave

$$\Delta E_{1/2} = E_{1/2}{}^k - E_{1/2} = -\frac{RT}{nF} \ln K_{eq} - \frac{xRT}{nF} \ln a(C_2H_4) \tag{7}$$

potential in eq 7 is the midpoint between the peak anodic and cathodic currents of a particular scan.

$$E_{1/2} = \frac{E_{pa} + E_{pc}}{2} \tag{8}$$

For a one-electron ($n = 1$) reversible process at room temperature, eq 7 becomes

$$\Delta E_{1/2} = -0.0591 \log K_{eq} - 0.0591x \log a(C_2H_4) \tag{9}$$

From the observed value of the shift in the half-wave potential $\Delta E_{1/2}$ (also called the formal potential difference), the value of K_{eq} can be estimated for the complexation of ethylene in solution. For $K_{eq} > 1$, larger

negative values of $\Delta E_{1/2}$ mean the system has a larger ability to absorb ethylene.

For the divalent copper [corresponding to the Cu(II)/Cu(I) couple], the direction of electron transfer from the cuprous ion is opposite from the previous derivation. This leads to a shift in the half-wave potential given by

$$\Delta E_{1/2} = E_{1/2}{}^{k} - E_{1/2} = \frac{RT}{nF} \ln K_{eq} + \frac{xRT}{nF} \ln a(C_2H_4) \tag{10}$$

For a one-electron ($n = 1$) reversible process at room temperature

$$\Delta E_{1/2} = 0.0591 \log K_{eq} + 0.0591x \log a(C_2H_4) \tag{11}$$

When $K_{eq} > 1$, a shift of the formal potential difference of greater than zero ($\Delta E_{1/2} > 0$) corresponds to an increase in the absorptivity of ethylene by this chemical system.

For these nonaqueous solutions, coordinating ligands were used to stabilize and solvate the metal ions. The equilibrium reactions contain additional exchange reactions due to the competition between the ligands and the olefin for the metal ion. Generally, p ligands are required to coordinate the copper ion given by

$$Cu^+ + pL \leftrightarrow Cu^+L_p \tag{12}$$

where L is either the anion or an organic ligand. Reaction 12 is assumed to occur quickly and completely so that essentially all metal ions are coordinated. When an ethylene molecule is introduced into the system, it can either add to the metal−ligand complex or replace an existing ligand. If the ethylene adds to the complex, the coordination number of the metal will increase and a new geometry will arise, but the estimation of the corresponding K_{eq} from eq 9 is the same.

$$Cu^+L_p + xC_2H_4 \leftrightarrow Cu^+L_p(C_2H_4)_x \tag{13}$$

If the ethylene replaces an existing ligand, the complex can retain its original structure with the cleavage of a metal−ligand bond and the formation of the metal−olefin bond.

$$Cu^+L_p + xC_2H_4 \leftrightarrow Cu^+L_{p-x}(C_2H_4)_x + xL \tag{14}$$

The displaced ligand creates a different form of the equilibrium equation that changes the calculation of K_{eq} for the Cu(I)/Cu(0) couple.

$$\Delta E_{1/2} = -0.0591 \log K_{eq} - 0.0591x \log \frac{a(C_2H_4)}{a(L)} \tag{15}$$

The additional term in eq 15 makes the calculation of K_{eq} much more difficult without prior knowledge of the interaction between the anion and other ligands with the metal ion. The coordination number (including whether the anion behaves as a coordinating ligand) and the structure of the complex would be necessary to proceed without direct measurement of the ligand concentration. Relatively weak ligands are easily replaced by incoming ethylene, but stronger ligands or ligands present in high enough concentrations create a competition with ethylene for coordination sites. This competition for the metal can lead to reduced capacity when solvent molecules can act as ligands or when ligands are too strong for ethylene to compete.

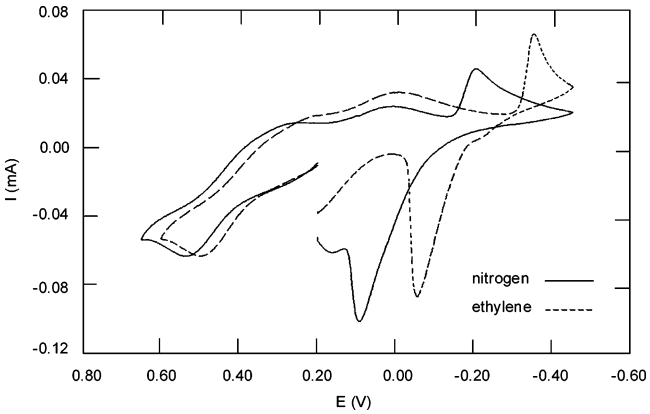

Figure 3. CV curve of nonaqueous 0.01 M CuCl with 0.4 M aniline at 100 mV/s. The features on the left at about 0.40 V correspond to the Cu(II)/Cu(I) couple, while those on the right between 0.20 and −0.50 V correspond to the Cu(I)/Cu(0) couple.

Table 1. CV Data at Given Scan Rates and Ligand Concentrations for the Cu(I)/Cu(0) Couple

		$\Delta E_{1/2}$ (mV, ±2)			
		CuCl		CuBr	
ligand	scan rate, mV/s	0.05 M py	0.40 M py	0.05 M py	0.40 M py
pyridine	20	−58	−30	−23	−32
	50	−60	−33	−31	−35
	100	−63	−35	−30	−34
	200	−64	−30	−28	−30
	1000	−58	−24	−23	−31

		$\Delta E_{1/2}$ (mV, ±2)			
		CuCl		CuBr	
ligand	scan rate, mV/s	0.05 M BzA	0.40 M BzA	0.05 M BzA	0.40 M BzA
BzA	20		−32		−16
	50	−63	−30	−44	−14
	100	−57	−26	−38	−11
	200	−50	−29	−30	−8
	1000	−52	−67	−39	−6

		$\Delta E_{1/2}$ (mV, ±2)			
		CuCl		CuBr	
ligand	scan rate, mV/s	0.40 M an	4.0 M an	0.40 M an	4.0 M an
aniline	20		−150		
	50	−147	−139	−152	10
	100	−147	−148	−143	−5
	200	−147	−146	−136	−11
	1000	−141	−154	−129	−16

Results and Discussion

CV. The change in potential due to ethylene treatment was recorded over a range of scan rates. The results as formal shifts in the half-wave potential ($\Delta E_{1/2}$) are presented in Table 1 at the range of scan rates used. The system with the best capacity for ethylene absorption was comprised of cuprous chloride with aniline. The CV curve for CuCl with aniline is shown in Figure 3, where the shift in the formal potential is seen as the difference between the peaks for the ethylene (dashed line) over the nitrogen (solid line), where both the cathodic and anodic peaks for the Cu(I)/Cu(0) couple exhibit large shifts. At low ligand concentrations, both

chloride and bromide systems exhibit a two-step redox process, meaning that the Cu(II)/Cu(I) and Cu(I)/Cu(0) couples are distinguishable in the voltammogram as in Figure 3. For these cases, only the Cu(I)/Cu(0) data are shown in Table 1.

From the CV data, the coordinating ability of the ligands studied increases in the following order: aniline $\ll$ pyridine $<$ BzA. If the cuprous ion coordinates with a stronger ligand such as BzA, ethylene molecules show a lesser degree of complexation as seen by the smaller negative shifts in the formal potential. By examination of both the chloride and bromide cases for a ligand concentration of 0.4 M, the shifts in the formal potential increase from BzA to pyridine to aniline following the coordination strength from greatest to least. If a ligand is strongly coordinating, then it will show its greatest ethylene capacity at the concentration nearest its coordination ratio with the metal ion. However, increases in the ligand concentration show a reduced ethylene capacity due to the binding tendency of the ligand, making it difficult for the olefin to compete for the metal. This trend is significant for BzA, with the shift in the formal potential decreasing (from -57 to -26 mV for CuCl and from -38 to -11 mV for CuBr at a 100 mV/s scan rate) when the ligand concentration is increased from 0.05 to 0.4 M. If a ligand is weakly coordinating like aniline, it will not show the reduction in the ethylene capacity at ligand concentrations over its coordination number. For example, the cuprous chloride and aniline case shows essentially no change in shift in the formal potential (given as -147 and -148 mV at a 100 mV/s scan rate) from 0.4 to 4.0 M, corresponding to ligand-to-metal ratios of 40:1 and 400:1, which are well in excess of the normal range of the coordination number (2−5) for copper(I) complexes in solution.[9] The strong ligand concentration effect is important because a large concentration of a strong ligand can impede the absorption process. Determining the best ligand can be difficult because if the ligand is too strong, it will hinder the ethylene substitution reaction (eq 14). If the ligand is too weak, the ligand will not fully complex the metal ion, leading to a more destabilized copper, which will likely have poor solubility and hence yield a solvent with poor olefin capacity.

The effect of the anion is similar to that of the coordinating ligand. The chloride ion was observed to be a weaker anion than the bromide ion. By examination of the 0.05 M pyridine systems for the two anions, the chloride case shows over double the shift in the formal potential as the bromide case. Another example of the anion exhibiting the same type of behavior as ligands can be seen in the aniline systems. Because aniline is a weak ligand, the coordinating effect of the counterion becomes more significant. With the weak chloride ion, the ethylene capacity is nearly independent of the aniline concentration. As a result, even a high concentration of the weak ligand does not reduce the copper's complexing ability because the chloride ion is easily replaced and incoming ethylene molecules have no problem exchanging with the weak aniline ligands. For the opposite case, a strong anion does not surrender as easily, which is evident by the cuprous bromide system's remarkable drop in shift in the formal potential for the more concentrated aniline case. Therefore, the inhibitory effect seen with strong ligands is also present even with weak ligands because one of the coordinating sites on the copper ion is lost to the stronger bromide ion.

With stronger ligands, it is more difficult to observe this anion effect because the behavior can be attributed to the ligand strength as mentioned above. In fact, this concentration/anion effect argument does not hold true for the pyridine−cuprous bromide system. This system surprisingly retains its ethylene-binding ability at 0.4 M pyridine over 0.05 M pyridine. An additional experiment was performed with cuprous bromide using excess pyridine as the solvent, which still showed a considerable shift in the formal potentials of up to -28 mV for the highest scan rate. It is unclear why the pyridine−CuBr system does not show a decreased capacity for higher ligand concentrations especially when the trend is observed with the chloride case.

The trend that the chloride anion formed weaker complexes than the bromide complexes is consistent with the hard and soft acid and base prediction for the stability of metal−halide complexes ($F < Cl < Br \ll I$).[10] This order has been confirmed for ethylene adsorption on solid CuCl and CuBr both experimentally[11,12] and theoretically (for a monocoordinated surface).[13] However, solution studies with other metals such as rhodium and iridium suggest the opposite trend.[14−16]

Autoclave. To validate the results of the CV experiments for concentrated metal systems, all six systems were prepared at about 1 M copper concentration in an inert-atmosphere glovebox. The solutions were desired to be at least 1 M in copper with a ligand-to-copper ratio of 4:1 because Cu(I) ions typically favor four-coordinate complexes.[9,17,18] For the BzA−CuBr and aniline−CuBr solutions, the prepared solution precipitated crystals while cooling to room temperature, requiring additional dilution with solvent to completely dissolve all of the crystals. The final calculated copper molarities of the BzA−CuBr and aniline−CuBr solutions were 0.57 and 0.93 M, respectively, while the calculated copper molarities of the other solutions ranged from 1.10 to 1.18 M. A brief return to the discussion of the bromide versus chloride ions and their interaction with copper complexes is helpful. The observed lower solubility of the two bromide cases suggests that the solvent solvates the coordinating ligands and does not necessarily complex with the cation. The solutions with low solubility were Br systems with both a strong ligand (BzA) and a weak ligand (aniline). Therefore, solubility is not a function of the ligand strength but the degree that the ligand is able to fully coordinate the cation without being obstructed by strong anions. It is not surprising that the CV results indicated that bromide systems exhibited poorer ethylene complexation because the bromide ions are more likely to hold tightly to the copper cation than their chloride counterparts and thus disable a potential ethylene−ligand exchange site.

After a prepared solution was introduced into the autoclave, a gas charge from the gas bomb was allowed to equilibrate with the liquid at ambient temperature. The time to reach equilibrium was usually between 1 and 3 h. The pressure decrease was analyzed to produce an equilibrium point on the plot of pressure versus ethylene concentration in liquid. The effect of activity coefficients is not considered here because related results confirmed them to have little physical relevance to the complexation equilibrium. A combination of multiple absorption experiments at different gas charges yields the curve observed in Figure 4 for a given system. From Figure 4, the aniline systems were observed to show the highest ethylene absorption followed by a close

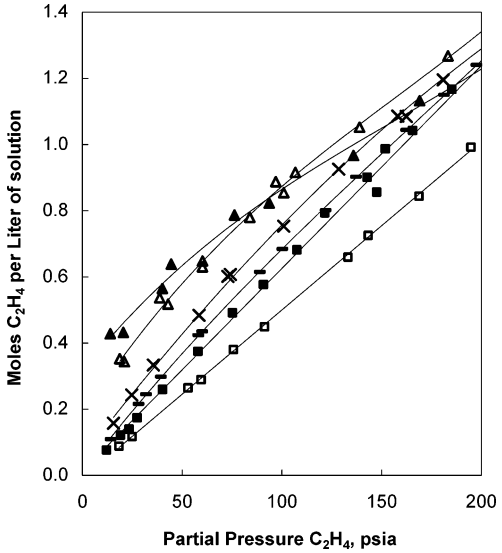

Figure 4. Ethylene loading as a function of the ethylene partial pressure for all six systems: (▲) ethylene in aniline−DMF−CuCl; (△) ethylene in aniline−DMF−CuBr; (×) ethylene in BzA−DMF−CuCl; (—) ethylene in BzA−DMF−CuBr; (■) ethylene in pyridine−DMF−CuCl; (□) ethylene in pyridine−DMF−CuBr.

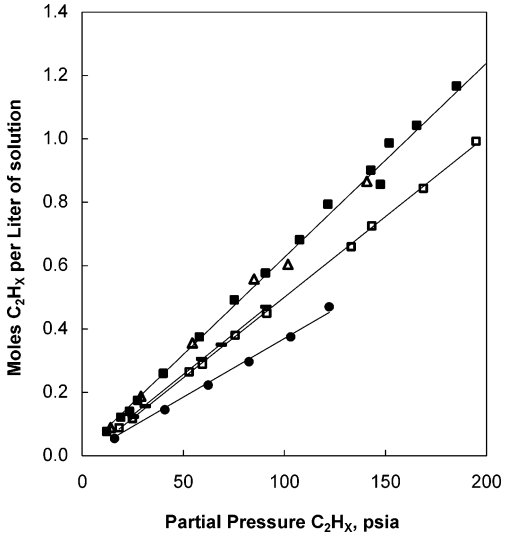

Figure 5. Physical solubility and salt effect: (■) ethylene in pyridine−DMF−CuCl; (△) ethylene in pyridine−DMF; (—) ethane in pyridine−DMF; (□) ethylene in pyridine−DMF−CuBr; (●) ethylene in pyridine−DMF−CuCl.

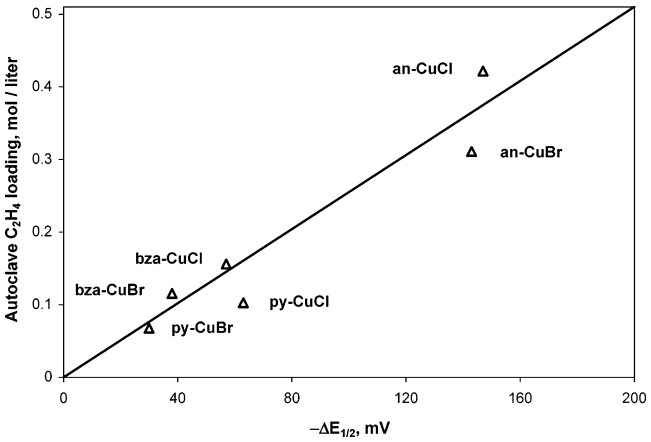

Figure 6. Parity plot of the CV half-wave potential at a 100 mV/s scan rate for lower ligand concentrations and autoclave ethylene loadings at 1 atm of ethylene pressure (the diagonal line is drawn to show a qualitative comparison).

grouping of BzA and pyridine systems at lower ethylene absorption. The autoclave and CV techniques are consistent in the fact that aniline far outperforms the systems of pyridine and BzA. Another commonality with CV is the fact that the chloride systems show higher absorption than the bromide systems for all autoclave cases. The shape of the equilibrium lines in Figure 4 can be seen to increase in curvature from bottom (lower ethylene absorption) to top (higher ethylene absorption). The pyridine systems show a linear dependence on pressure, suggesting a strong physical solubility effect of the solvent. Unlike the CV experiments where the observed complexation was strictly chemical, the autoclave experimental results do not isolate the chemical effects from the physical effects, so the observed absorption is a combination of the two phenomena.

To further examine the role of physical solubility in the absorption equilibrium curves, a new solution was prepared with an equivalent molar ratio of pyridine and DMF without the copper salt. Because the pyridine−CuCl and pyridine−CuBr systems experienced physical solubility, they should also have experienced the salting-out effect: changes in physical solubility after the addition of a salt. The salt effect was best demonstrated by an additional series of experiments with ethane gas for the pyridine−CuCl system and the copper-free pyridine system. The pyridine−CuCl run with ethane shown in Figure 5 exhibited the salting-out effect. The capacity for ethane was clearly lower than the line produced from the copper-free case. The pyridine−CuCl run with ethylene did not appear to demonstrate salting out because that line was nearly the same as the line produced from the copper-free run with ethylene; however, the runs with pyridine−CuBr did exhibit the salt effect. The CuCl system should have experienced a similar effect, but because the CuCl line was higher than the CuBr line, the argument could be made that the CuCl system experienced more chemical effects than the CuBr system. The chemical effects may have compensated for the loss of physical solubility raising the CuCl line, which incidentally was in the same position as the copper-free line. The salt effect hypothesis should be tested with a solution of a nonreacting salt. A possibility would be to prepare a solution identical with pyridine−CuCl except to use NaCl (or KCl) instead of CuCl. The new salt should not participate in any chemical absorption, so the resulting equilibrium curve should show the pure salt effects on the physical absorption. Ideally, this new solution should exhibit an ethylene capacity slightly lower than that of the pyridine−CuBr case.

One of the main goals of this work was to determine whether the absorption capacities of concentrated systems could be qualitatively defined from dilute solutions in a bench-scale electrochemical experiment. If the total absorption observed in the autoclave is compared to the shift in the half-wave potential from the CV experiments, a parity plot suggesting a good fit is obtained in Figure 6. However, from all of the preceding discussions of the large amount of physical solubility and possible salt effects inherent in the autoclave, such a comparison may be potentially misleading. For example, the pyridine−CuBr absorption equilibrium curve is linear, with a zero intercept implying practically no chemical effects. The pyridine−CuCl system shows some chemical effects if the salt effect is assumed to be similar. However, it is not likely that the chemical effects would persist to

high ethylene loadings, as suggested by the fact that the equilibrium line has the same slope at very high pressures as it has at low pressures. The different slopes of the equilibrium line for the chloride and bromide cases especially at higher loadings can also be seen with aniline (except in this case the bromide has the greater slope). Possibly the chloride ion has some interaction that would cause a different degree of salting out than the bromide ion. Regardless of the explanation, the pyridine−CuCl system, like the bromide system, is also linear with a zero intercept. When compared to CV, these two systems should be best represented by zero chemical effects.

It is apparent that the autoclave equilibrium data contain a large dependency on the physical solubility of the different ligands and their molarities. For example, in both pyridine systems, a large portion of a system's total absorption capacity is due to physical solubility, so a system that has slightly more or less ligand compared to solvent will show a different capacity even though the chemical effects remain unchanged. Because the ligand and solvent have different physical solubilities for ethylene, a change in their ratio will change the degree of absorption of the solution. Varying these factors would cause the corresponding points on the parity plot in Figure 6 to fluctuate accordingly.

One reason for the poor chemical absorption of the strong ligand systems (pyridine especially) could be the strong ligand concentration effect. Even though the ligand-to-copper ratio in the autoclave was around 4:1, while the CV experiments were at 5:1 and 40:1, the higher overall concentration of the autoclave solution could account for the difference. Simple solution thermodynamics can be used to show that the dilute 0.01 M copper solution will not encounter as many ligand molecules at a 5:1 ratio as the 1.1 M copper solution at a 4:1 ratio. In addition, the actual coordination number of the metal−ligand complex could be less than the assumed value. Pyridine−CuCl complexes have been shown to have a binuclear structure with halide bridges so that each copper ion is four-coordinated but only at a ligand-to-metal ratio of 2.[19]

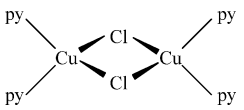

If the actual ligand-to-metal ratio for the complex were 2 instead of 4 as previously assumed, then the excess ligand concentration for the concentrated copper case would impede ethylene complexation as observed for the CV cases with higher strong ligand concentrations.

Conclusion

A benchtop electrochemistry technique was used to study six chemically different olefin absorption systems at two concentrations. These six systems were prepared at nearly saturated copper concentrations and evaluated by autoclave experiments to quantify olefin capacity. By using the Nernst equation, the shift in the formal potential is directly correlated to the system's equilibrium or capacity to absorb ethylene. Despite the difference of over 2 orders in magnitude in the copper concentration between the two techniques, validation of CV's predictive ability for absorption trends, although not quantitative, was seen to be qualitatively sound. The obvious trends predicted by CV were observed in the autoclave experiments (such as aniline's higher absorption than other ligands and chloride's higher absorption than bromide). Both techniques confirm that weak ligands with weak anions exhibit the greatest olefin capacity, and these systems should be the focus of further study as potential reactive absorption solvents.

Acknowledgment

We acknowledge the support of the Robert A. Welch Foundation for support of a fellowship (B.W.).

Nomenclature

Symbols

Δ = shift in potential due to complexation
° = standard reduction potential
1/2 = half-wave potential
k = complex

Characters

$a(x)$ = activity of species x
Cu = reduced copper metal
Cu^+ = copper ion not complexed to ethylene (other ligands not shown)
$Cu^+(C_2H_4)$ = copper−ethylene complex (other ligands not shown)
C_2H_4 = physically dissolved ethylene in solution
e = electron
E = electronic potential energy (V)
F = Faraday constant
K_{eq} = complexation reaction equilibrium constant
L = ligand molecule or anion
n = number of electrons transferred in the redox reaction
p = coordination number of the ligand
R = gas constant
T = temperature
x = coordination number of ethylene

Literature Cited

(1) Ethylene. In *Ullman's Encyclopedia of Industrial Chemistry*, 5th ed.; Gerhartz, W., Ed.; VCH Verlagsgesellschaft: Weinheim, Germany, 1987; Vol. A10, pp 45−93.

(2) Eldridge, R. B. Olefin/Paraffin Separation Technology: A Review. *Ind. Eng. Chem. Res.* **1993**, *32*, 2208−2212.

(3) Safarik, D. J.; Eldridge, R. B. Olefin/Paraffin Separations by Reactive Absorption: A Review. *Ind. Eng. Chem. Res.* **1998**, *37*, 2571−2581.

(4) Kim, C. J.; Palmer, A. M.; Milliman, G. E. Absorption of Carbon Monoxide into Aqueous Solutions of K_2CO_3, Methyldiethanolamine, and Diethylethanolamine. *Ind. Eng. Chem. Res.* **1988**, *27*, 324−328.

(5) Jamal, A.; Meisen, A. Kinetics of CO induced degradation of aqueous diethanolamine. *Chem. Eng. Sci.* **2001**, *56*, 6743−6760.

(6) Smith, J. M.; Van Ness, H. C.; Abbott, M. M. *Introduction to Chemical Engineering Thermodynamics*, 5th ed.; McGraw-Hill: New York, 1996.

(7) Monk, P. *Fundamentals of Electro-Analytical Chemistry*; John Wiley & Sons: Chichester, U.K., 2001.

(8) Galus, Z. In *Fundamentals of Electrochemical Analysis*; Marcinkiewicz, S., Translator; Reynolds, G. F., Ed.; Halsted: New York, 1976.

(9) Munakata, M.; Kitagawa, S. The Chemistry of Copper(I) Complexes in Solution. In *Copper Coordination Chemistry: Biochemistry and Inorganic Perspectives*; Karlin, K. D., Zubieta, J., Eds.; Adenine: New York, 1983; pp 473−495.

(10) Pearson, R. G. Hard and Soft Acids and Bases. *J. Am. Chem. Soc.* **1963**, *85*, 3533−3539.

(11) Long, R. B. Separation of Unsaturates by Complexing with Solid Copper Salts. In *Recent Developments in Separation Science*; Li, N. N., Ed.; CRC: Boca Raton, FL, 1972; Vol. 1, pp 35−57.

(12) Gilliland, E. R.; Seebold, J. E.; FitzHugh, J. R.; Morgan, P. S. Reaction of Olefins with Solid Cuprous Halides. *J. Am. Chem. Soc.* **1939**, *61*, 1960−1962.

(13) Chen, J. P.; Yang, R. T. A Molecular Orbital Study of the Selective Adsorption of Simple Hydrocarbon Molecules on Ag^+- and Cu^+-Exchanged Resins and Cuprous Halides. *Langmuir* **1995**, *11*, 3450−3456.

(14) Forster, D. Relative Stabilities of Some Halide Complexes of Rhodium and Iridium. *Inorg. Chem.* **1972**, *11*, 1686−1687.

(15) Brady, R.; Flynn, B. R.; Geoffroy, G. L.; Gray, H. B.; Peone, J., Jr. Electronic Spectral Studies of Planar Rhodium(I) and Iridium(I) Complexes Containing π-Acceptor Ligands. *Inorg. Chem.* **1976**, *15*, 1485−1488.

(16) Branan, D. M.; Hoffman, N. W.; McElroy, A.; Miller, N. C.; Ramage, D. L.; Schott, A. F.; Young, S. H. Anion Affinity of Carbonylbis(triphenylphosphine)rhodium(I) in CH_2Cl_2: Fluoride vs Its Halide Analogues. *Inorg. Chem.* **1987**, *26*, 2915−2917.

(17) Haase, D. J. Process for Removal of Selected Component Gases from Multicomponent Gas Streams. U.S. Patent 5,382,417, 1995.

(18) Lewin, A. H.; Michl, R. J.; Ganis, P.; Lepore, U.; Avitabile, G. Copper(I) Complexes: Synthesis and Crystal Structure of Tetrapyridine Copper(I) Perchlorate $(C_5H_5N)_4CuClO_4$. *J. Chem. Soc., Chem. Commun.* **1971**, 1400−1401.

(19) Kitagawa, S.; Munakata, M. Binuclear Copper(I) Complexes Which Reversibly React with CO. 1. Di−μ-halogeno-bis(2,2′-bipyridine)dicopper(I) and Its Derivatives. *Inorg. Chem.* **1981**, *20*, 2261−2267.

Received for review January 28, 2004
Revised manuscript received June 18, 2004
Accepted July 20, 2004

IE049917N